Materials Characterization 121 (2016) 157–165

Contents lists available at ScienceDirect

Materials Characterization

journal homepage: www.elsevier.com/locate/matchar

Microstructure and partitioning behavior characteristics in low carbon steels treated by hot-rolling direct quenching and dynamical partitioning processes

Yun-jie Li, Xiao-lei Li, Guo Yuan *, Jian Kang, Dong Chen, Guo-dong Wang

State Key Laboratory of Rolling and Automation, North Eastern University, Shenyang, China

ARTICLE INFO

Article history:
Received 23 May 2016
Received in revised form 4 October 2016
Accepted 5 October 2016
Available online 06 October 2016

Keywords:
DQ&P process
Proeutectoid ferrite
Retained austenite
Carbon concentration
Mechanical property

ABSTRACT

In this work, a new process and composition design are proposed for "quenching and partitioning" or Q&P treatment. Three low carbon steels were treated by hot-rolling direct quenching and dynamical partitioning processes (DQ&P). The effects of proeutectoid ferrite and carbon concentration on microstructure evolution and mechanical properties were investigated. The present work obtained DQ&P prototype steels with good mechanical properties and established a new notion on compositions for Q&P processing. Microstructures were characterized by means of electro probe microanalyzer (EPMA), scanning electron microscopy (SEM), electron backscatter diffraction (EBSD), transmission electron microscopy (TEM) and X-ray diffraction (XRD), especially the morphology and size of retained austenite. Mechanical properties were measured by uniaxial tensile tests. The results indicated that introducing proeutectoid ferrite can increase the volume fraction of retained austenite and thus improve mechanical properties. TEM observation showed that retained austenite included the film-like inter-lath austenite and blocky austenite located in martensite/ferrite interfaces or surrounded by ferrites. It was interesting that when the carbon concentration is as low as ~0.078%, the film-like inter-lath untransformed austenite cannot be stabilized to room temperature and almost all of them transformed into twin martensite. The blocky retained austenite strengthened the interfaces and transformed into twin martensite during the tensile deformation process. The PSEs of specimens all exceeded 20 GPa.%.

1. Introduction

With the rapid development of automobile industry, the lightweight and safety of automobile steels are emphasized [1]. Hence, the advanced high strength steel (AHSS) has become a focus recently [2], because of its good combination of strength and ductility. Quenched and partitioned steel (Q&P) [3–5] proposed by Speer et al. in 2003 is a representative one of AHSS including the following sequences. Firstly, the steel is full or partly austenitized and then quenched to a pre-determined temperature (QT) in between the martensite-start temperature (Ms) and the martensite-finish temperature (Mf) to form a microstructure consisting of martensite, ferrite (if the steel was intercritically austenitized) and untransformed austenite. Then, the steel is either isothermally held at QT (which is called 1-step partitioning) or brought to a higher partitioning temperature (PT) (2-steps) allowing carbon to diffuse from the supersaturated martensite into the untransformed austenite. As a result of carbon enrichment during partitioning step, the Ms. of the untransformed austenite is lowered. In this way, the metastable austenite is retained in the steel after the final quenching to the room temperature. This cycle aims at producing microstructures consisting of carbon-depleted martensite and retained austenite which possess good comprehensive properties due to the high strength of martensite and the TRIP effect of retained austenite [6,7].

In traditional Q&P concept, the experimental materials with concentrations of C higher than 0.2 (wt.%) are considered to be appropriate for Q&P processing and in this way, much more retained austenite could be obtained. In fact, depending on the steel chemistry and the Q&P treatments parameters, there exist competing reactions during partitioning procedure, such as bainite [8,9] and carbides formation [10], even in low-carbon steels [8] and in high-carbon steels [11,12], even when containing a high amount of Si [13]. The competing reactions are disadvantageous to enrich retained austenite, and this proved that the amount of retained austenite did not only depend on carbon concentration and not all the carbon was used to stabilize austenite. Hence, the lower carbon steels may also be appropriate for Q&P processing and a desired amount of retained austenite may be obtained through the coupling effects of original microstructure and partitioning procedure.

Recently, most of the studies about Q&P steel focused on obtaining high strength steels by designing high carbon or high alloy composition, however, the elongation of the steels is always lower than 20%. The mismatch of strength and elongation leads to bad formability and some

* Corresponding author.
E-mail address: yuanguoral@sina.com (G. Yuan).

http://dx.doi.org/10.1016/j.matchar.2016.10.005
1044-5803/

Table 1
Chemical compositions (wt.%) and critical temperature (°C) of the experimental steels.

Steel	C	Si	Mn	Ae3	Ms
A	0.19	1.60	1.60	846	398
B	0.12	1.55	1.55	868	429
C	0.078	1.55	1.61	887	447

problems in application. Generally, low carbon Si-Mn steel without other alloying elements was difficult to obtain high PSE (product of strength and elongation). However, some recent investigations noted that Q&P steels with proeutectoid ferrite possessed low yield strength and good elongation which lead to improvement of comprehensive mechanical properties, but the effects of proeutectoid ferrite are not clear yet, especially in low carbon steel. Furthermore, the traditional Q&P treatment mainly focused on the hot-rolling off-line Q&P treatment and the Q&P treatment of cold-rolled sheet, resulting in high energy consumption and complex heat treatment processes. In recent years, the directly quenching and partitioning (DQ&P) [14] process has attracted many researchers' attentions. Compared with traditional Q&P treatment, DQ&P has the following advantages [14,15]: 1) The directly quenching after deformation can make the best of the residual heat for partitioning, which is more simplified and energy-efficient. 2) The combination of DQ&P process and thermo mechanical control process (TMCP) is favorable to obtaining the desired microstructure and good mechanical properties. 3) High density dislocation and fine grains can improve the mechanical properties, such as work hardening capacity, strength and elongation. 4) It can save alloy elements. Moreover, the present research mainly focuses on isothermal partitioning procedure. For matching to the thermal process characteristics of hot strip mill processing, where there is no capability for either reheating or isothermal partitioning, the investigation of dynamical partitioning process proposed by Thomas [12] is of importance. The dynamical partitioning process is considered to be a good way for carbon diffusion. And it means that the quenching temperature is equal to coiling temperature and serves as initial partitioning temperature.

In this work, in order to study the effect of the dynamical partitioning process in low carbon steels on the microstructure evolution, three low carbon steels were treated by DQ&P process. In addition, the influence of the proeutectoid ferrite on different features of the retained austenite and their impacts on the mechanical properties were also investigated.

2. Experimental Procedure and Materials

The chemical compositions of the steels used in this study are listed in Table 1. Steels were melt in a vacuum induction furnace and then forged into a billet with the section dimension of 60 mm × 40 mm. The critical temperature of Ae_3 was calculated by Thermo-calc 5.0 and Ms. was calculated by empirical formula [16]. The schematic thermal profiles of the processes are illustrated in Fig. 1. Three processes have the same austenization and hot rolling procedures. But process 1 represents direct water quenching after hot rolling (HR) and then coiling from the QT. Process 2 includes air cooling process after hot rolling, water quenching to QT and coiling from the QT. Process 3 includes air cooling process after hot rolling and water quenching to room temperature. The partitioning step occurs during coiling from the quenching temperature to room temperature. Specifically, the slabs were austenized at 1200 °C for 1.5 h and then hot-rolled from 40 mm to 18 mm thickness though 2 passes at about 1120 °C. When air-cooled to 920 °C, the plates were again hot-rolled to 4 mm though 4 passes with a finish rolling temperature about 880 °C.·Then the five plates underwent different heat treatment processes (see Table 2).

The tensile samples with dimensions of 12.5 mm in width, 4 mm in thickness and 50 mm in length were prepared along the rolling direction and tested on a CMT5105-SANS machine at room temperature with an extension rate 2 mm/min. The ultimate tensile strength (UTS), 0.2% yield strength (YS) and elongation were obtained based on the average of three tests for each plate.

The distributions of elements of selected specimen were investigated by a JXA-8530F electro probe microanalyzer (EPMA) equipped with energy dispersive X-ray spectrum (EDS) system at an operating voltage of 20 kV, current of 2×10^{-8}A and a step size of 40 nm. The microstructure characterization was carried out using a Zeiss Ultra-55 filed emission scanning electron microscope (SEM) equipped with an electron backscattered diffraction (EBSD) system. The EBSD technique was used to identify the present phases. For observations of fine structure of microstructure, transmission electron microscope (TEM) investigation was carried out using a TECNAL G220 microscope at an operating voltage of 200 kV. For SEM and EPMA observation, the specimens were grounded and etched by 4% nital for 10–15 s. The specimens for EBSD analyses with a step size of 40 nm were firstly grounded and then electro-polished using electrolyte containing alcohol, perchloric acid and water with a proportion of 13:2:1 at room temperature. The current is about 1.2 A and the time is about 25 s for electro-polishing process. The TEM specimens were firstly grounded to a thickness of 45 μm and then electro-polished at −20 °C in a twin-jet machine.

The amount and average carbon concentration of residual austenite were measured at room temperature by a D/max2400X-ray diffractometer (operated at 56 kV, 182 mA) with Cu Kα radiation at room temperature. The test surfaces along the rolling direction were electro-polished to eliminate the stress of surface. And samples were scanned over a 2θ range from 40° to 110° with a step of 0.04°/s including several important ferrite and austenite peaks. The integrated intensity of ferrite peaks of (200), (211) and austenite peaks of (200), (220) and (311) were used to calculate the volume fraction of austenite by Jade version

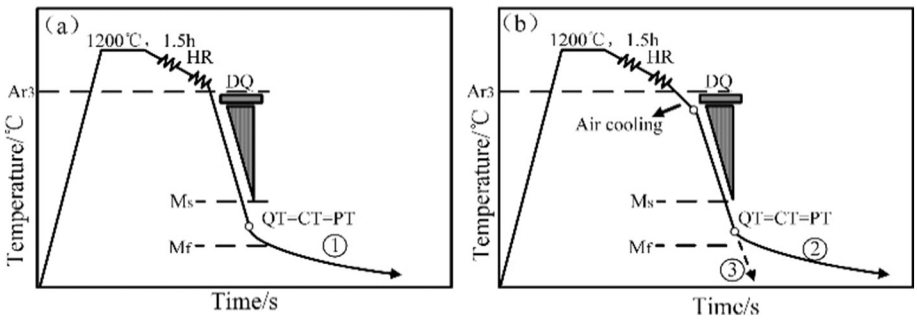

Fig. 1. Schematic thermal profiles of the process: Compared with process (a), the process (b) includes air cooling, aiming at introduction of proeutectoid ferrite. The specimens for process 1 and 2 were cooled inside the furnace to room temperature and the coiling cooling rate was about 60 °C/h for partitioning. "Ar3"represents the temperature of ferrite formation in the cooling process of prior austenite. "HR" means hot rolling. "DQ" means directly quenching. "QT" means quenching temperature. "CT" means coiling temperature. "PT" means initial partitioning temperature.

Table 2
Heat treatment parameters of steels: Austenization 1200 °C < 1.5 h>, finishing rolling temperature at 880 °C and water quenching are equal to all samples. "T" means temperature.

Steel	Sample	Process	Air cooling process	T before quenching	Quenching T
A	No. 1	1	NO	880 °C	280 °C
A	No. 2	2	YES	760 °C	280 °C
A	No. 3	3	YES	760 °C	RT
B	No. 4	2	YES	760 °C	330 °C
C	No. 5	2	YES	830 °C	230 °C

Table 3
Amount of proeutectoid ferrite and RA and carbon concentration in RA.

Sample	Percentage of proeutectoid ferrite (%)	Percentage of RA (%)	Carbon concentration in RA (wt.%)
No. 1	0	8.5	0.9
No. 2	25.0	11.3	1.3
No. 3	25.4	4.5	1.0
No. 4	62.0	10.2	1.2
No. 5	52.2	6.0	1.1

6.5. The amount of retained austenite was obtained by the following equation [17]:

$$V_\gamma = 1.4I_\gamma/(I_\alpha + 1.4I_\gamma) \quad (1)$$

where V_γ, I_γ and I_α are the volume of retained austenite, the average integrated of the (200), (220) and (311) austenite peaks and average integrated of the (200) and (211) ferrite peaks, respectively.

The average carbon concentration of retained austenite was calculated using the following equation [18]:

$$C_\gamma = (\alpha_\gamma - 3.547)/0.046 \quad (2)$$

where the C_γ is the austenite carbon concentration in weight percent and the α_γ is the lattice parameter of the austenite in Angstroms calculated using Eq. (3). The (220) and (311) of austenite peaks were chose to calculate the α_γ.

$$a_\gamma = \frac{\lambda\sqrt{h^2+k^2+l^2}}{2\sin\theta} \quad (3)$$

where λ,(*hkl*), and θ are the wavelength of the radiation, the three Miller indices of a plane and the Bragg angle, respectively.

3. Results and Discussion

3.1. The Effects of Proeutectoid Ferrite and Carbon Concentration on Stabilizing Retained Austenite

As can be seen in Fig. 2, the typical microstructure of specimen No. 1 is lath martensite. Compared with specimen No. 1, specimen No. 2 containing about 25% (see Table 3) proeutectoid ferrite has smaller martensite packets which are benefit to improvement of strength and ductility. And the martensite structure of specimen No. 3 is not clear, since it is as-quenched. In Fig. 2a, there exist some carbides distributing in martensite, and this may be attributed to the tempering during long-time coiling, while specimen No. 2 containing proeutectoid ferrite seems to have less carbides as in Fig. 2b. As can be seen, specimen No. 4 and No. 5 with lower carbon concentration contain more ferrite, 62.0% and 52.2%, respectively and finer martensite packets.

The distributions of carbon in steel A are shown in Fig. 3. It is obvious that the carbon distributions are non-uniform. From Fig. 3a, carbon enriched zones can be observed between the martensite laths indicating that carbon has diffused from supersaturated martensite to untransformed austenite during the dynamical partitioning step. As for specimen No. 2, besides martensite laths, the carbon enriched at proeutectoid ferrite boundaries (Fig. 3b), indicating that the proeutectoid ferrite can promote inhomogeneous carbon distributions. By contrast, specimen No. 3 was directly quenched to the room temperature without partitioning step, the carbon of which only enriched at proeutectoid ferrite boundaries. It is more likely to obtain more retained austenite and produce low carbon steels with good comprehensive

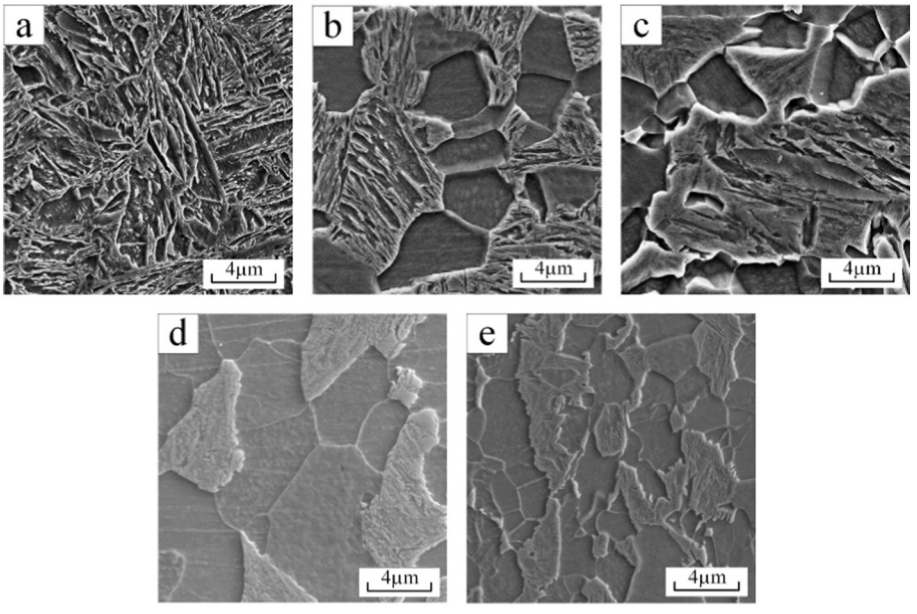

Fig. 2. SEM micrographs of specimens: (a) No. 1; (b) No. 2; (c) No. 3; (d) No. 4; (e) No. 5.

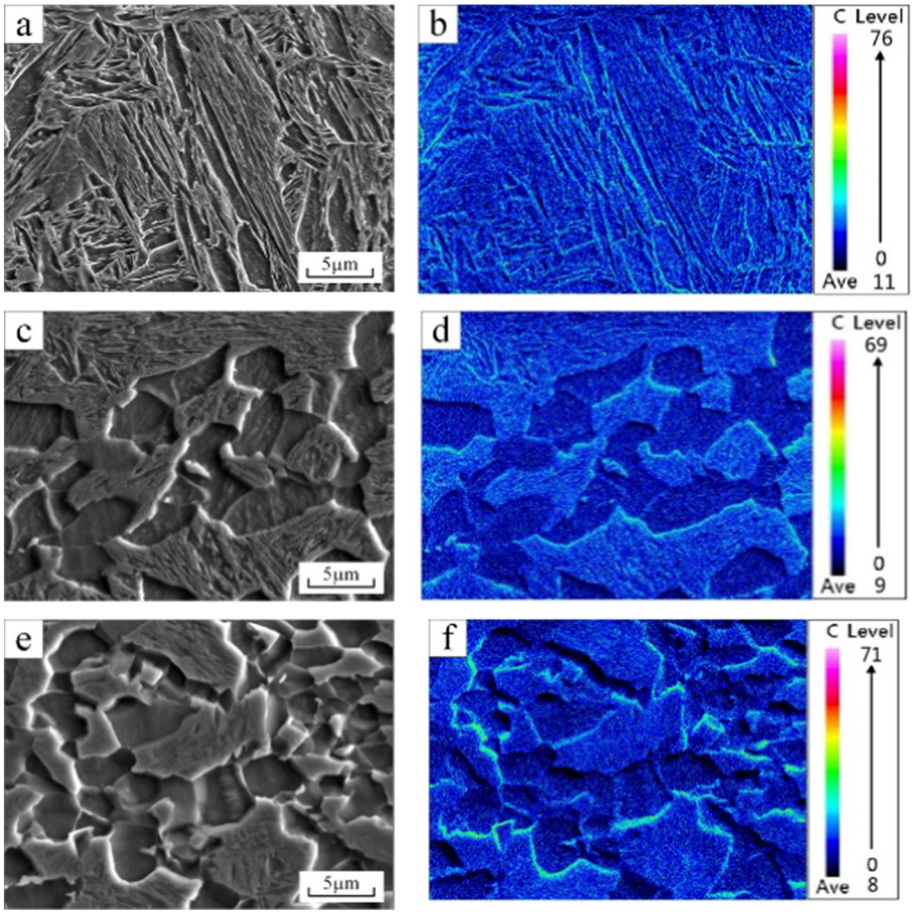

Fig. 3. Elements distributions in the tested specimens: (a) secondary electro image for No. 1; (b) carbon distribution for No. 1; (c) secondary electro image for No. 2; (d) carbon distribution for No. 2; (e) secondary electro image for No. 3; (f) carbon distribution for No. 3.

properties by introducing a proper amount of proeutectoid ferrite. In this study, the distributions of Mn and Si are uniform and not presented. Note that the inhomogeneous states caused by proeutectoid ferrite will be limited by carbon concentration of steels. This will be analyzed in the following part.

In order to investigate the couple effects of proeutectoid ferrite and dynamical partitioning on distribution, morphology and amount of retained austenite, the dynamically partitioned specimen No. 2 was chose for EBSD analyzing. Fig. 4 shows that retained austenite distributes in martensite inter-lath, ferrite grain boundaries and ferrite/martensite interfaces. The retained austenite in martensite inter-lath is more likely to be film while that in boundaries or interfaces is blocky. As mentioned in some researches, the morphologies and distributions of untransformed austenite have large effects on their partitioning [19–21]. Firstly, the smaller austenite grain size has greater potential to absorb carbon atoms from its surrounding phases because of the larger interfacial area between the austenite and its adjacent phases per austenite volume, which can accelerate carbon partitioning by offering more tunnels for diffusion. Then, duo to hydrostatic pressure of initial martensite, the film-like untransformed austenite between martensite laths tends to be stabilized easier and thus create a relative low carbon in the film-like retained austenite. Because of the limited EBSD step size of 40 nm, some retained austenite cannot be detected. The accurate amount of retained austenite was measured by XRD experiment. Fig. 5 shows that three specimens have different intensity of austenite peaks and the austenite peaks of specimen No. 2 are most obvious. After

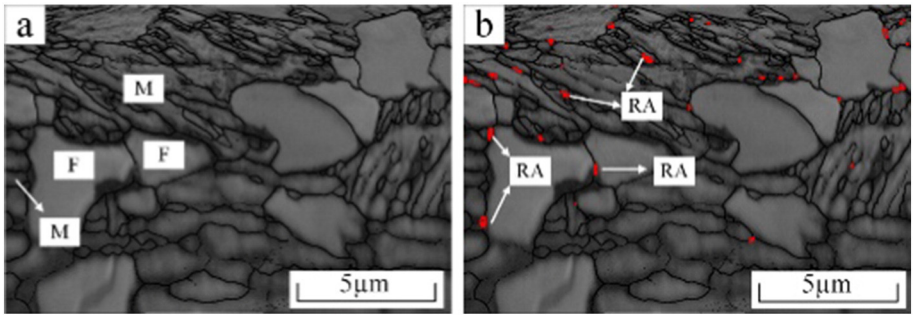

Fig. 4. EBSD analysis results of the microstructures of the tested No. 2: (a) combined band-contrast map and grain boundaries; (b) image quality maps combining with retained austenite (the red part). "M" martensite. "F" means ferrite. "RA" means retained austenite. (For interpretation of the references to colour in this figure legend, the reader is referred to the web version of this article.)

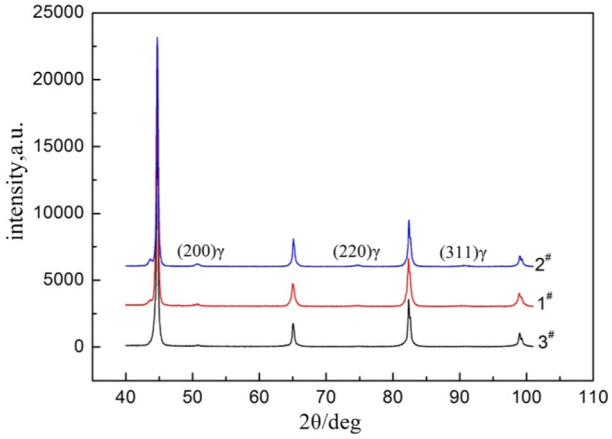

Fig. 5. Results of X-ray diffraction peaks of the tested specimens.

being calculated, the percentages of retained austenite in specimen No. 1, No. 2 and No. 3 are 8.5%, 11.3% and 4.5%, respectively (see Table 3). The maximum retained austenite is reached in No. 2, indicating proeutectoid ferrite is helpful to obtain more retained austenite. The average carbon concentration in retained austenite are 0.9%, 1.3% and 1.0%, respectively. The features of carbon concentration in retained austenite are in agreement with the previous studies [21], reflecting that the film-like austenite has a lower average carbon concentration. It is not difficult to understand. The film-like austenite is located in martensite laths, where carbide precipitation is often observed during the partitioning step. The carbide consumes amount of carbon, reducing the remaining amount of carbon that is used to enrich austenite, thus resulting in a relative low carbon concentration in film-like austenite. The austenite in ferrite grain boundaries or ferrite/martensite interfaces tends to have a higher carbon concentration, since it possesses a large amount of carbon from proeutectoid ferrite and plentiful defects of interfaces providing path for carbon diffusion from supersaturated martensite to blocky untransformed austenite. The major approach to stabilize the austenite is to promote the enrichment of the relevant elements, leading to its Ms. below room temperature, as shown by the following equation [16]:

$$\mathrm{Ms}(^{\circ}\mathrm{C}) = 539 - 423\mathrm{C} - 30.4\mathrm{Mn} - 7.5\mathrm{Si} + 30\mathrm{Al} \quad (4)$$

One can conclude that the most effective approach to stabilize retained austenite is to promote the carbon enrichment. But, it is not the main method, the size [22–25] and morphology [26–28] of austenite also played an important role. In this work, for steel A, only when the carbon concentration of untransformed austenite exceeds 1.072%, the Ms. would drop below room temperature (25 °C). However, it is surprising in specimen No. 1, the average carbon concentration is 0.9%, which proves that less carbon was needed to stabilize the film-like untransformed austenite. This is because that the film-like untransformed austenite has small size and strip shape. On the basis of the results, it is clear that more retained austenite can be obtained by decreasing prior austenite size through heavy compressive deformation, controlling the size and morphology of untransformed austenite or introducing a right amount of ferrite for steel B or steel C.

Although the carbon concentrations of specimen No. 4 and No. 5 are relatively lower, 0.12%, 0.078%, respectively, the retained austenite was obtained. This is mainly because that the prior austenite were partitioned by abundant ferrites, thus resulting in finer martensite laths and untransformed austenite. After being calculated, the percentages of retained austenite for specimen No. 4 and No. 5 are 10.2% and 6.0%, respectively. And the average carbon concentration of the retained austenite are 1.2% and 1.1%, respectively. It seems that all carbon was used to partition effectively, despite of the calculation errors. Anyhow, this result indicates that retained austenite can be obtained in steels with the relative lower carbon by combining introduction of ferrite with dynamical partitioning.

Fig. 6 shows two types of retained austenite morphologies in the specimen No. 2. The film-like retained austenite with a thickness between 20 nm and 60 nm shows N-W orientation relationship with the adjacent martensite laths according to the selected area electron diffraction patterns shown in Fig. 6(c). The blocky retained austenite includes two types. The austenite surrounded by ferrite is always polygonal with a thickness about 200 nm. The other austenite located in ferrite/martensite phase interfaces presents various morphologies: the closed

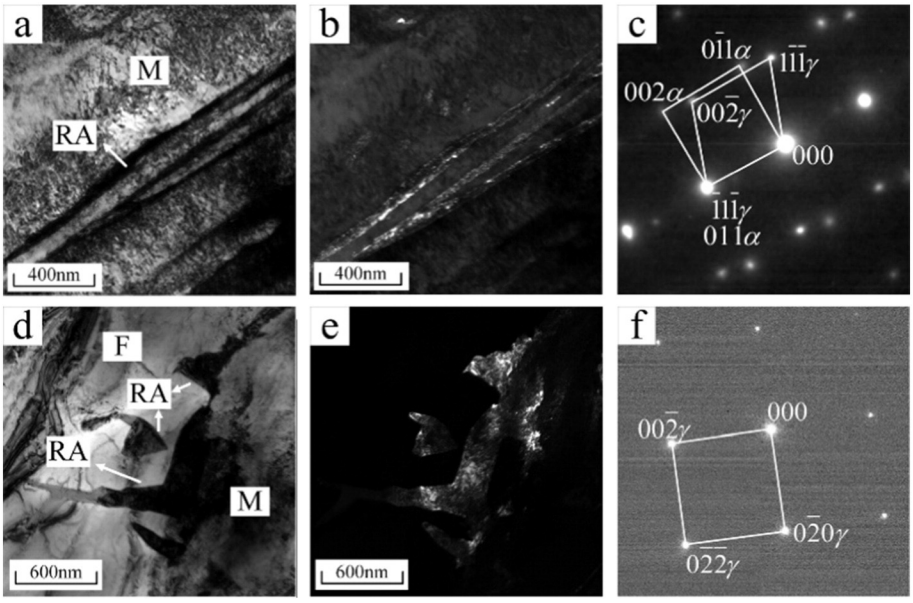

Fig. 6. TEM micrographs showing morphology and distribution of retained austenite of No. 2: (a) film-like austenite bright field; (b) film-like austenite dark field; (c) SAED pattern of both the martensite and the retained austenite; (d) blocky austenite bright field; (e) blocky austenite dark field; (f) SAED pattern of the retained austenite. "RA" means retained austenite. "M" means martensite.

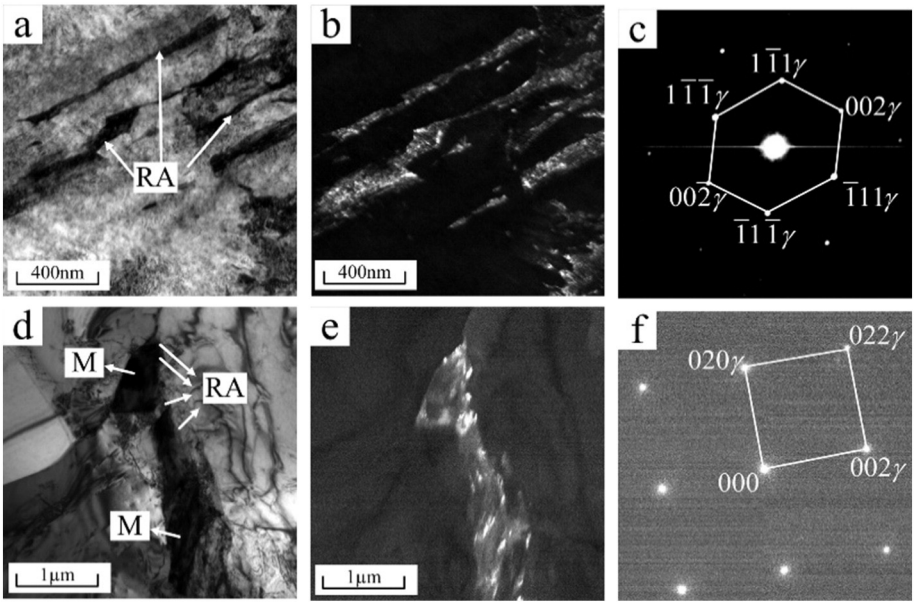

Fig. 7. TEM micrographs showing morphology and distribution of retained austenite of No. 4: (a) film-like austenite bright field; (b) film-like austenite dark field; (c) SAED pattern of the retained austenite; (d) blocky austenite bright field; (e) blocky austenite dark field; (f) SAED pattern of the retained austenite. "RA" means retained austenite. "M" means martensite.

angle part with a thickness about 100 nm spreading inside of ferrite and the bigger part distributing in ferrite/martensite phase interfaces. Because of the high carbon concentration of steel A, the blocky retained austenite is mainly continuous. However it is also found that a very small amount of untransformed austenite has transformed into martensite, indicating that the carbon concentration in an austenite region is non-uniform especially in specimen No. 4 and No. 5 (Figs. 7 and 8). As mentioned in some previous literatures [21], the carbon concentration is also not uniform among austenite regions. This is attributed to two reasons. Firstly, carbon enrichment of prior austenite is inhomogeneous during the formation of proeutectoid ferrite. Secondly, the untransformed austenite has different morphology and size after quenched. The smaller austenite grain size has a larger interfacial area with its surrounding phases per austenite volume resulting in a good ability to absorb carbon atoms from adjacent phases during partitioning step. Based on the above, the smaller blocky untransformed austenite and austenite beside proeutectoid ferrite have high carbon concentration and they are easier to be stabilized to room temperature.

The retained austenite of specimen No. 4 and No. 5 was observed by TEM (as Fig. 8 shows). Besides typical film-like retained austenite, the blocky retained austenite is also observed in specimen No. 4. Different from that in No. 2, the blocky retained austenite in No. 4 presents a long strip shape with 200 nm in width and is not continuous, where the part located in ferrite/martensite phase interfaces or ferrite grain boundaries is retained and the center area of untransformed austenite has transformed into martensite. Comparing with specimen No. 2 and No. 4, the film-like retained austenite in specimen No. 5 cannot be obtained and many twin martensites are observed between martensite laths. In addition, the blocky retained austenite in specimen No. 5 was difficult to distinguish and it had smaller grain size, only distributing by the side of ferrite/martensite phase interfaces or ferrite grain boundaries. This indicates that the carbon from adjacent martensite laths was

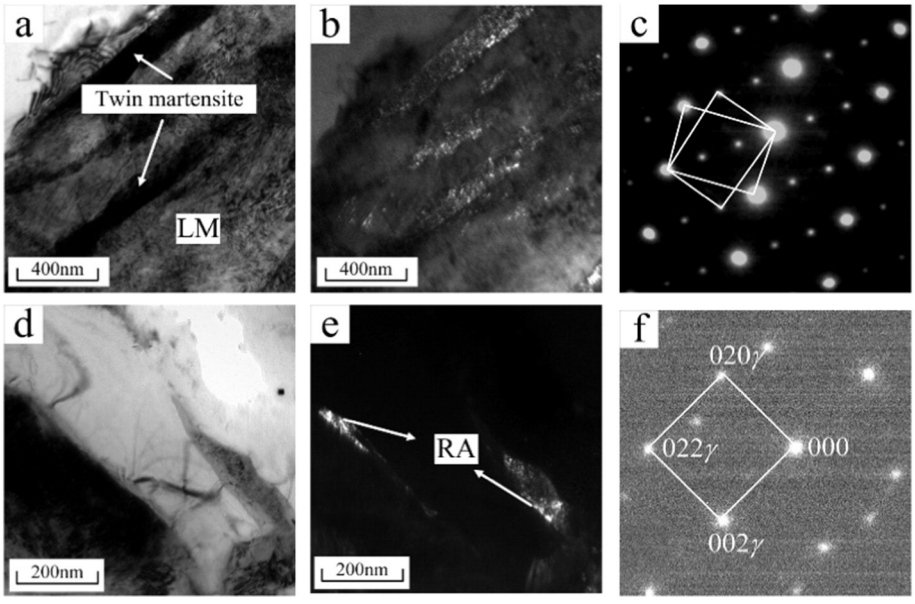

Fig. 8. TEM micrographs showing morphology and distribution of retained austenite of No. 5: (a) twin-martensite bright field; (b) twin-martensite dark field; (c) SAED pattern of the twin-martensite; (d) blocky austenite bright field; (e) blocky austenite dark field; (f) SAED pattern of the retained austenite. "LM" means lath martensite. "RA" means retained austenite.

Table 4
Mechanical properties.

Specimen	Yield strength (MPa)	Tensile strength (MPa)	Yield ratio	Elongation (%)	Product (GPa.%)
1#	985	1247	0.79	13.37	16.666
2#	605	1070	0.56	21.4	22.900
3#	648	1110	0.59	8.83	9.870
4#	495	875	0.57	25.58	22.380
5#	470	845	0.56	24.85	21.000

not sufficient in steel C, resulting in that most of untransformed austenite transformed into twin martensites during dynamical partitioning step. And the stability of austenite caused by proeutectoid ferrite is limited.

For steels with low carbon concentration, such as steel B or steel C, if carbon concentration is uniform in an austenite region during proeutectoid ferrite formation, the austenite region is more likely to transform into martensite during quenching or partitioning step. This is because that the carbon concentration is not enough to make the austenite region stabilized to room temperature. But in most cases, the carbon concentration is non-uniform in an austenite region before quenching and that in ferrite/martensite phase interfaces or ferrite grain boundaries is rich in carbon, which can be stabilized to room temperature. Besides, the prior austenite grain size will be divided by a large amount of ferrite grains in specimen No. 4 and No. 5. In this case, there is more untransformed austenite with the right morphology and size for partitioning after quenching, which is key to obtaining retained austenite in steel B and steel C. Although the stability of austenite caused by proeutectoid ferrite is limited, it is promising to obtain appropriate microstructure by adjusting the amount of proeutectoid ferrite and controlling quenching temperature for the sake of producing steels with good comprehensive properties.

3.2. The Relationship of Retained Austenite and Mechanical Properties

The mechanical properties are shown in Table 4. The YS and yield ratio of specimen No. 1 are very high, reaching 985 MPa and 0.79 respectively. But the elongation is only 13.37%, which leads to its bad formability and low PSE. By introducing a certain amount of proeutectoid ferrite into specimen No. 2, the YS decreases to 605 MPa and the reduction of the UTS is 177 MPa, but the elongation increases by 7.03% reaching up to 21.4%, making PSE increase to 22.900 GPa.% from 16.666 GPa.%. Similarly, the PSEs of specimen No. 4 and No. 5 both exceed 20.000 GPa.% and the PSE of No. 4 reaches 22.380 GPa.%. It is difficult to get such a good comprehensive property in such a low carbon steel. The high elongation is not only attributed to proeutectoid ferrite, but also attributed to the large amount of retained austenite. In addition, both of specimen No. 4 and No. 5 have low yield ratio. Although ferrite will slightly sacrifice UTS, it has many advantages. Firstly, Q&P steel containing a certain amount of ferrite owns a low yield ratio, ensuring its good formability [9]. Further, the proper amount of ferrites can obtain a large scale enhancement of elongation, the reasons of which include two aspects: 1) firstly, as soft phase, ferrite has good plasticity. 2) the ferrite increases the amount of retained austenite, enhancing TRIP effect.

It is generally known that the blocky retained austenite has better chemical stability because of its higher carbon concentration. It is necessary to make clear TRIP effect of blocky retained austenite and thus the discussion is as following. Fig. 9 shows the retained austenite states of both the un-deformed and deformed tested specimens. Before deformation, the carbon in retained austenite is between 0.9% and 1.3% similar to previous researches [19,29]. But for specimen No. 2 and 4, the carbon concentration in retained austenite is above 1.2%, and even as high as 1.3%. This is due to the coupling effects of introducing proeutectoid ferrite and dynamic partitioning. The fraction of retained austenite in deformed specimens is between 2.0% and 3.0%, indicating that most of retained austenite has transformed to martensite during deformation. For specimen No. 2 and 4, nearly 8.0% retained austenite has transformed to martensite, resulting in a good elongation >20%. In comparison, the elongation of specimen No. 1 is only 13.37%, since it contained no ferrite and the lower amount of retained austenite. The carbon concentration in deformed specimens maintained a high level >1.4%, indicating that most of retained austenite with relatively lower carbon concentration has transformed into martensite, especially that in the specimen No. 2 and 4. In fact, the blocky retained austenite has a larger volume, so it has larger grain boundary area providing more nucleation sites for martensite transformation during deformation. Due to the characteristics of blocky retained austenite, only a small part that contains extremely high carbon cannot paly TRIP effect, as the specimen No. 2 and No. 4 show.

The TEM graphs of selected deformed specimens are shown in Fig. 10. After deformation, many twin martensites (as the arrows point) can be observed in the M/F interfaces or the zones surrounded by proeutectoid ferrites. That is to say, the blocky retained austenite has transformed into twin martensite during deformation, despite of its higher carbon concentration. This was reported in the previous paper [21]. Because of the insufficient carbon concentration in untransformed austenite, a small amount of twin martensite was also formed in the first quenching or partitioning step. Furthermore, most of film-like retained austenite also has transformed into martensite, but it is difficult to distinguish it from martensite laths. A recent study [21] has shown that the film-like retained austenite was more stable and it deformed relatively later. The facts that lath martensite has a high yield stress and a high hydrostatic pressure suppresses its martensitic transformation. The crack nucleation, crack propagation and the deformation environment can give a better explanation and will be discussed in the following part.

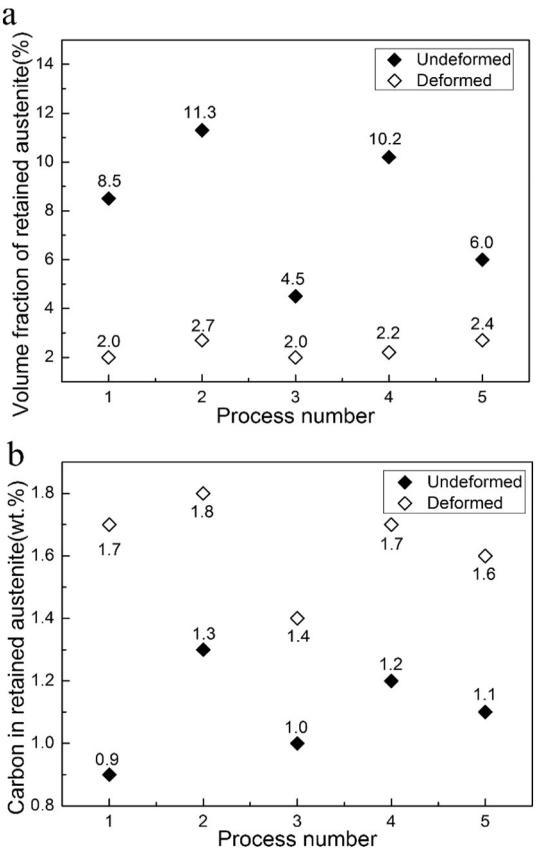

Fig. 9. Retained austenite states of both the un-deformed and deformed (fractured) tested specimens.

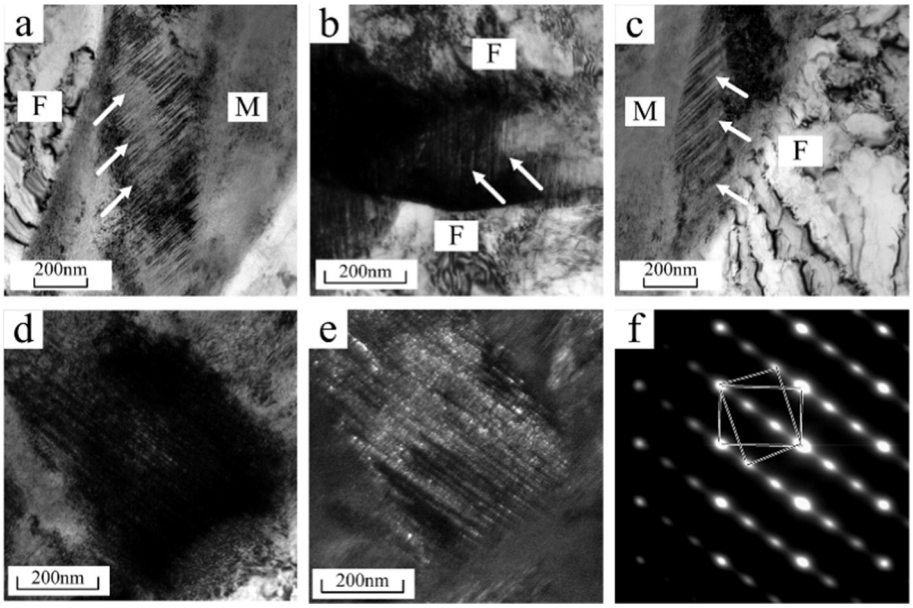

Fig. 10. TEM investigation of selected deformed specimens: (a) twin martensite of deformed No. 2; (b) twin martensite of deformed No. 4; (c) twin martensite of deformed No. 5; (d) twin martensite bright field of No. 2; (e) twin martensite dark field of No. 2; (f) SAED pattern of the twin martensite. "F" means ferrite. "RA" means retained austenite.

In order to clarify the tensile fracture mechanism, the micro-cracks in the specimen No. 2 were investigated by SEM, as shown in Fig. 11. There are two types of crack nucleation. Generally, F/M interfaces possess higher energy, so they are preferred positions for crack nucleation, as can be seen in Fig. 11(c). Another position for crack nucleation is the interior of ferrite grains (Fig. 11b). It is worth mentioning that Q&P steels containing proeutectoid ferrite are different from dual-phase steels. The micro-cracks of dual-phase steels are easy to form in the ferrite/martensite phase interfaces, due to their big differences in physical characters between martensite and ferrite. However, for Q&P steels, the coupling effects of introducing proeutectoid ferrite and the partitioning step make much different size or morphology retained austenite exist in the ferrite/martensite phase interfaces, resulting in a smaller hardness gradient interfaces relative to previous ferrite/martensite phase interfaces. Because of this, the brittleness of ferrite/martensite phase interfaces of Q&P steels can be remitted effectively. That way, the micro-cracks are more difficult to form in phase interfaces.

Fig. 11(a) shows the propagation path of a crack. The point a represented the fracture position of the sample. From point a to b, the crack firstly propagated along the ferrite/martensite phase interfaces and then propagated cross a ferrite grain. At the moment, the crack propagation path must be changed because of the TRIP effect of blocky retained austenite located in the interfaces and the hard tempered martensite. Then the crack propagation will repeated the above processes. When the stress was sufficiently high, the crack propagated into martensite and ceased to extend at a definite depth, as point d shows. Sometimes, because of insufficient stress, some cracks also stop propagating in ferrite grains, as Fig. 11(b) and (c) show. In this study, the sufficient

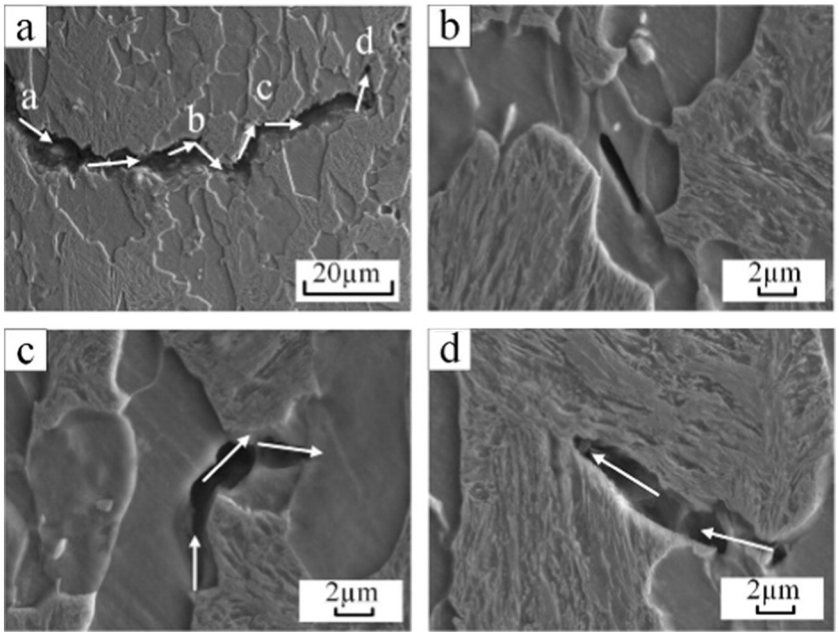

Fig. 11. The observation of cracks propagation for No. 2.

grain boundaries of grain refinement of the rolling deformation and the abundant phase interfaces would be the barriers for crack propagation. Thereby, the crack cannot keep propagating straightly and must change its path. Consequently, the crack propagation rate is slowed and that is the reason why Q&P steels containing some proeutectoid ferrite have good plasticity and toughness. In a word, introducing a certain amount of proeutectoid ferrite into Q&P steels is conducive to enhancing mechanical properties. Moreover, PSEs can be further improved by adding micro-alloy elements such as Nb, V, Ti or adjusting the quenching temperature. But there is also a question needing to be solved that how much the film-like and blocky retained austenite is, respectively and how to evaluate their sole donation to mechanical properties. This will be analyzed in the future work.

4. Conclusion

In this paper, three low carbon steels were treated by hot rolling direct quenching and dynamical partitioning processes. The microstructure, especially the amount and morphologies of retained austenite, mechanical properties and the relationship of retained austenite and tensile fracture behavior were investigated. The results showed that introduction of proeutectoid ferrite can obtain more retained austenite and thus improve the comprehensive mechanical properties. The retained austenite and high PSEs were obtained, even in 0.078%C steel and 0.12%C steel. This indicated that steel for Q&P processing need not contain concentrations of carbon higher than 0.2%. In this study, the retained austenite includes two morphologies: one is film-like interlath austenite located in martensite laths and another is blocky austenite distributing in ferrite grains boundaries or ferrite/martensite phase interfaces. But, the couple effects of introducing proeutectoid ferrite and dynamical partitioning are limited by carbon concentration. When carbon concentration is as low as 0.078%, film-like retained austenite cannot be obtained and only a small amount of blocky retained austenite can be stabilized to room temperature, therefore the 0.078%C steel might not be suitable for Q&P processing and the steel with carbon concentration higher than 0.1% should be considered. Tensile results indicated that the blocky retained austenite improved the ferrite/martensite grain boundaries and most of retained austenite has transformed to martensite during tensile deformation, which is the key to obtaining high PSEs. In addition, this work also proved that carbon partition can be accomplished during dynamical partitioning step and the DQ&P process is promising in the industry production.

Acknowledgments

This work was funded by the National Basic Research Program of China (no. 51504063), the Natural Science Foundation of Liaoning Province of China (no. 2014020027).

References

[1] S. Zhou, K. Zhang, Y. Wang, J.F. Gu, Y.H. Rong, High strength-elongation product of Nb-microalloyed low-carbon steel by a novel quenching–partitioning–tempering process, Mater Sci Eng A 528 (2011) 8006–8012.
[2] X.D. Wang, Z.H. Guo, Y.H. Rong, Mechanism exploration of an ultrahigh strength steel by quenching–partitioning–tempering process, Mater Sci Eng A 529 (2011) 35–40.
[3] J.G. Speer, D.K. Matlock, B.C. De Cooman, J.G. Schroth, Carbon partitioning into austenite after martensite transformation, Acta Mater 51 (2003) 2611–2622.
[4] J.G. Speer, D.V. Edmonds, F.C. Rizzo, D.K. Matlock, Partitioning of carbon from supersaturated plates of ferrite, with application to steel processing and fundamentals of the bainite transformation, Curr. Opin. Solid State Mater. Sci. 8 (2004) 219–237.
[5] J.G. Speer, E. De Moor, K.O. Findley, D.K. Matlock, B.C. De Cooman, D.V. Edmonds, Analysis of microstructure evolution in quenching and partitioning automotive sheet steel, Metall. Mater. Trans. A 42A (2011) 3591–3601.
[6] B.C. De Cooman, Structure–properties relationship in TRIP steels containing carbide-free bainite, Curr. Opin. Solid State Mater. Sci 8 (2004) 285–303.
[7] S.G. Liu, S.S. Dong, F. Yang, et al., Application of quenching–partitioning–tempering process and modification to a newly designed ultrahigh carbon steel, Mater. Des. 56 (2014) 37–43.
[8] M.J. Santofimia, L. Zhao, J. Sietsma, Microstructural evolution of a low-carbon steel during application of quenching and partitioning heat treatments after partial austenitization, Metall. Mater. Trans. A 40 (2009) 46–57.
[9] N. Zhong, X.D. Wang, Y.H. Rong, et al., Interface migration between martensite and austenite during quenching and partitioning (Q&P) process, J. Mater. Sci. Technol. 22 (06) (2006) 751–754.
[10] Y. Toji, G. Miyamoto, D. Raab, Carbon partitioning during quenching and partitioning heat treatment accompanied by carbide precipitation, Acta Mater 86 (2015) 137–147.
[11] D.V. Edmonds, K. He, F.C. Rizzo, et al., Quenching and partitioning martensite—a novel steel heat treatment, Mater Sci Eng A 438–440 (2006) 25–34.
[12] Y. Toji, H. Matsuda, M. Herbig, et al., Atomic-scale analysis of carbon partitioning between martensite and austenite by atom probe tomography and correlative transmission electron microscopy, Acta Mater 65 (2014) 215–228.
[13] H.K.D.H. Bhadeshia, D.V. Edmonds, The bainite transformation in a silicon steel, Metall. Mater. Trans. A 10 (1979) 895–907.
[14] M.C. Somani, D.A. Porter, L.P. Karjalaien, D.K. Misra, Evaluation of DQ&P processing route for the development of ultra-high strength tough ductile steels, J. Metall. Eng. 2 (2013) 154–160.
[15] X. Tan, Y. Xu, X. Yang, Z. Liu, D. Wu, Effect of partitioning procedure on microstructure and mechanical properties of a hot-rolled directly quenched and partitioned steel, Mater Sci Eng A 594 (2014) 149–160.
[16] J. Mahieu, J. Maki, B.C. De Cooman, et al., Phase transformation and mechanical properties of Si-free CMnAl transformation-induced plasticity–aided steel, Metall. Mater. Trans. A 33A (2002) 2573–2580.
[17] K.I. Sugimoto, N. Usui, M. Kobayashi, S.I. Hashimoto, Effects of volume fraction and stability of retained austenite on ductility of TRIP-aided dual-phase steels, ISIJ Int. 32 (1992) 1311–1318.
[18] K.I. Sugimoto, T. Iida, J. Sakaguchi, T. Kashima, Retained austenite characteristics and tensile properties in a TRIP type bainitic sheet steel, ISIJ Int. 40 (2000) 902–908.
[19] Y. Xu, X. Tan, X. Yang, et al., Microstructure evolution and mechanical properties of a hot-rolled directly quenched and partitioned steel containing proeutectoid ferrite, Mater Sci Eng A 607 (2014) 460–475.
[20] C.Y. Wang, J. Shi, W.Q. Cao, et al., Characterization of microstructure obtained by quenching and partitioning process in low alloy martensitic steel, Mater Sci Eng A 527 (2010) 3442–3449.
[21] X.C. Xiong, B. Chen, M.X. Huang, et al., The effect of morphology on the stability of retained austenite in a quenched and partitioned steel, Scripta Mater. 68 (2013) 321–324.
[22] D.Q. Bai, A. Di Chiro, S. Yue, Stability of retained austenite in a Nb microalloyed Mn-Si TRIP steel, Mater Sci Forum 284–286 (1998) 253–262.
[23] E. Jimenez-Melero, N.H. van Dijk, L. Zhao, J. Sietsma, S.E. Offerman, J.P. Wright, S. van der Zwaag, Characterization of individual retained austenite grains and their stability in low-alloyed TRIP steels, Acta Mater 55 (2007) 6713–6723.
[24] H.-S. Yang, H.K.D.H. Bhadeshia, Austenite grain size and the martensite-start temperature, Scripta Mater. 60 (2009) 493–495.
[25] E. Jimenez-Melero, N.H. van Dijk, L. Zhao, J. Sietsma, S.E. Offerman, J.P. Wright, S. van der Zwaag, Austenite grain size and the martensite-start temperature, Scripta Mater. 56 (2007) 421–424.
[26] H.K.D.H. Bhadeshia, D.V. Edmonds, Bainite in silicon steels: new composition–property approach part 1, Metal Sci. 17 (1983) 411–419.
[27] A. Basuki, E. Aernoudt, Influence of rolling of TRIP steel in the intercritical region on the stability of retained austenite, J. Mater. Process. Tech. 89–90 (1999) 37–43.
[28] I. Timokhina, P. Hodgson, E. Pereloma, Effect of microstructure on the stability of retained austenite in transformation-induced-plasticity steels, Metal. Mater. Trans. A 35 (2004) 2331–2341.
[29] X. Tan, Y. Xu, X. Yang, et al., Effect of partitioning procedure on microstructure and mechanical properties of a hot-rolled directly quenched and partitioned steel, Mater Sci Eng A 589 (2014) 101–111.